Implementation of a Fourth-Order Compact Quasi-Elliptic Substrate Integrated Waveguide Filter in C-Band

Narges kiani[1,*], Majid Afsahi [2], Farzad Tavakkol Hamedani [3] and Pejman Rezaei[3]

Abstract— **Substrate Integrated Waveguide (SIW) technology by application of the planar construction process obtains a catchy means for integrating planar and nonplanar circuits. Further, it is hard to realize the negative coupling needed to create a compact quasi-elliptic bandpass filter based on a single-layered SIW structure. The presented work proposes a specific planar and negative coupling configuration that provides two transmission zeroes at 5.03 GHz and 6.26 GHz. This article presents a fourth-order quasi-elliptic filter. The proposed filter is also wide-band. This structure is implemented in SIW knowledge. The SIW filter has a central frequency of 5.5 GHz. The perfect bandwidth is 0.7 GHz. It is realized on a single-layer substrate from Rogers Ro4003. The Thickness of the substrate is considered as 0.508 mm. The measured outcomes of this filter, which show an excellent selectivity, and a low insertion loss of about 1.9 dB, agree suitably with simulation results. The designed filter's innovation provides these features: compact, low cost, wide-band, good selectivity, low insertion loss, and agreement between simulation and fabrication.**

Index Terms— **Substrate Integrated Waveguide (SIW), Quasi-Elliptic Filter, Band Pass Filter (BPF), Electric Coupling, Magnetic Coupling.**

I. INTRODUCTION

The rapid growth of communications services and devices happened lately [1, 2]. SIW technology has attracted a lot of consideration because of its benefits such as: low-cost fabrication, low loss, high-quality factor (Q-factor), high power handling capability, and easy integration. In comparison to multilayered SIW, single- layer SIW structures have more stuff. They include filters [3–18], antennas [19–21], and so on. The quasi-elliptic filters are trendy. Among the benefits of these filters, excellent out-of-band rejection is emphasized. Electric coupling (negative or cross-coupling) and magnetic coupling (positive or direct coupling) is applied in the structure of these types of SIW filters. In general, finite transmission zeroes (TZs) can be observed in the quasi-elliptic filter structures. However, mutual coupling between non-adjacent resonators is required to bring TZs from infinite to finite situations. It has been confirmed that both magnetic and electrical coupling is needed to generate TZs at limited frequency positions.

Furthermore, they obtain excellent selectivity in a cross-coupled filter. Generally, direct coupling is performed by using a magnetic post-wall window (positive coupling) in single-layered SIW filters. Usually, it is not easy to achieve negative coupling. BPF microstrip filters typically have a lower Q-factor compared to SIW filters. This is the basic weakness of BPF microstrip filters compared to SIW filters [22, 23]. There are electromagnetic excitations at the interface between metal and dielectric. These excitations are called surface plasmon polaritons (SPPs). Various devices based on SPPs have been reported. We can mention plasmonic filters among the tools that are very useful in this field. Unlike microwave filters, they cannot be manufactured, which is plasmonic filters' main weakness [24, 25].

In [3], a dual-mode SIW doublet bandpass filter was investigated using a CSRR. A SIW transversal filter using mixed source and load coupling was realized in [4]. In [5], a wide stopband SIW filter with corner cavities was explained. The multilayer technique was used to realize compact SIW filters in [6]. Analysis of SIW dual-band and broad stop-band filters were elaborated in [7]. A SIW filter based on a parallel-coupled microstrip line (PCML) reported [8]. A design system for SIW-EBG filters was reported in [9]. In [10], a study of SIW and HMSIW BPFs was presented by applying periodic configurations. Implementation of dielectric SIW filter by using two variant substrates proposed [11]. In [12], the performance of two different topologies of SIW BPFs was displayed in the S-band. The wide SIW BPFs were designed using stepped impedance structures [13]. A circular SIW BPF with a broad tuning range was studied in [14]. In [15], a compact SIW BPF was implemented by the compact microstrip resonant cell method. An investigation of the factors of the slow wave phenomenon on two species of miniaturized SIW BPFs was deduced in [16]. The access to H-plane SIW filters was introduced using propagative and evanescent modes in [17].

This paper presents a fourth-order SIW broadband filter. Both magnetic and electric couplings are used in the structure of this filter. The purpose of providing electric coupling is to reach an excellent coefficient and wide coupling stability range. The designed filter's innovation provides these features: compact, low cost, wide-band, good selectivity, low insertion loss, and agreement between simulation and fabrication. Simulations are implemented in CST Microwave Studio software [26].

1- Shariati Technical and Vocational College,Tehran, Iran.
2- Electrical and Computer Engineering Faculty, Semnan University, Semnan, Iran.
3- Electrical and Computer Engineering Faculty, Semnan University, Semnan, Iran.
Corresponding author: n.kiani@semnan.ac.ir

In section 2, the proposed filter coupling structure is presented, along with a detailed description of its coupling matrix. Section 3 describes the design features of the fourth-order bandpass filter. The simulation results of the designed structure are reported in Section 4. Finally, the fifth section presents the test and measurement results which are in suitable compromise with the simulation outcomes.

II. COUPLING MATRIX

The design of the fourth-order SIW filter is illustrated in Fig. 1.

The coupling diagram of the designed filter is remarkable in Fig. 2.
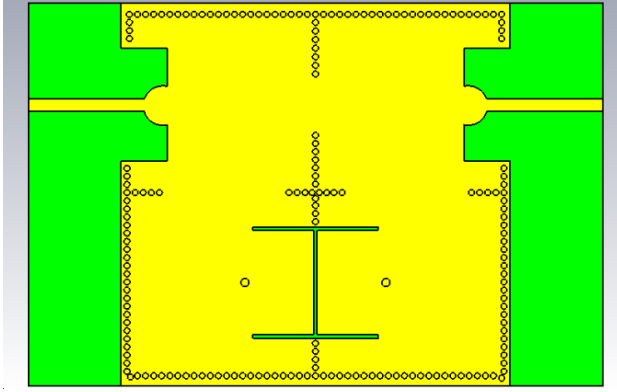
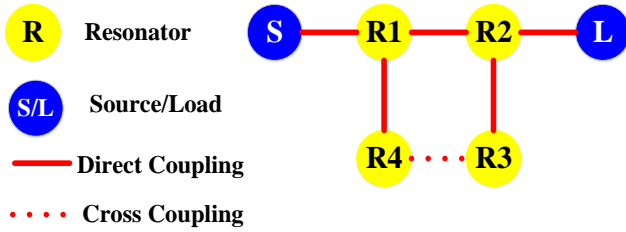Fig. 1. Configuration of the proposed structure.

Fig. 2. Coupling diagram.

In general, the coupling matrix is derived from Eq.1, which is as follows [27, 28]:

$$K_{ij} = K_{ji} = \frac{f_j^2 - f_i^2}{f_j^2 + f_i^2} \tag{1}$$

Applying Eq.1 to the proposed SIW filter structure yields this result. The cases k> 0 and k <0, are for magnetic coupling (direct coupling) and electric coupling (cross-coupling), respectively.

$$K_{ij} = \begin{bmatrix} +0.00 & +0.25 & +0.00 & +0.16 \\ +0.25 & +0.00 & +0.17 & +0.00 \\ +0.00 & +0.17 & +0.00 & -0.23 \\ +0.16 & +0.00 & -0.23 & +0.00 \end{bmatrix} \tag{2}$$

The K_{34} and K_{43} coupling coefficients are the same, and both are negative. The negative sign in the coupling coefficient displays TZs before and after the passband. These TZs are located at 5.03 and 6.256 GHz. Their position appears in the form of design results in future sections. The center frequency (f_0) of the SIW filter is located at 5.5686 GHz. The designed

SIW filter bandwidth (BW) is 0.7 GHz. This is how the generalized coupling matrix [29] is obtained, which is evident in Eq.3.

$$M_{ij} = K_{ij} \times \frac{f_0}{BW} = K_{ij} \times \frac{5.5}{0.7} = K_{ij} \times 7.9 \tag{3}$$

The generalized coupling matrix is given using Eq.3, matrix two, and the substitution of the values obtained from the filter frequency characteristic.

$$M_{ij} = \begin{bmatrix} +0.0 & +1.1 & +0.0 & +0.0 & +0.0 & +0.0 \\ +1.1 & +0.0 & +1.9 & +0.0 & +1.3 & +0.0 \\ +0.0 & +1.9 & +0.0 & +1.4 & +0.0 & +1.1 \\ +0.0 & +0.0 & +1.4 & +0.0 & -1.8 & +0.0 \\ +0.0 & +1.3 & +0.0 & -1.8 & +0.0 & +0.0 \\ +0.0 & +0.0 & +1.1 & +0.0 & +0.0 & +0.0 \end{bmatrix} \tag{4}$$

In the next step, the dimensions of the square cavity are approximated. To achieve this goal, the iris dimensions need to be modified. Such design adjustments are useful and appropriate to optimize coupling coefficients. In general, it can be said that this general rule applies to full-wave simulations of coupled cavities. The final step in designing is to adjust the dimensions of the cavities. The goal of implementing these proceedings is to repair the resonance movement created by the iris structure [27, 28]. The quality factor (Q_{ext}) is determined by Eq.5.

$$Q_{external} = \frac{f_0}{\Delta f_{\mp 90}} = 64.8 \tag{5}$$

In this Equation, the parameter $\Delta f_{\mp 90}$ is in the sense of bandwidth where the phase variation is ± 90 degrees [29].

III. FILTER DESIGN

The configuration of the proposed filter structure in CST software with the required design dimensions is illustrated in Fig. 3.

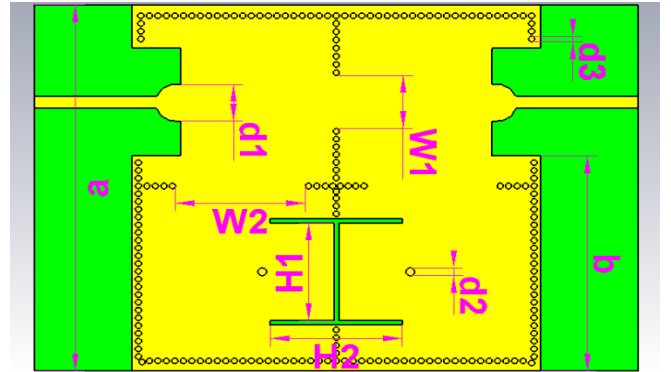The SIW filter dimension values are listed in Table I.

Fig. 3. Dimensions and configuration of the designed filter.

TABLE I
Designed Dimensions of the SIW Filter.

Designed Dimensions (in mm)			
a	b	W₁	W₂
33	20	5	11
d₁	d₂	d₃	H₁	H₂
4	0.7	0.5	9	11

The benefits of using fourth-order filters to achieve isolation are very high. The entire structure is implemented in a standard PCB process. The substrate is a Rogers RO4003. The substrate thickness is selected as 0.508 mm. The dielectric constant (ε_r) of this substrate is assumed to be 3.38. The value of loss tangent ($\tan \delta$) is also considered 0.0027. All sidewall vias should be drilled at a diameter of 0.5 mm. The central vias should be drilled at a diameter of 0.7 mm. The segmented filter structure is shown in Fig. 4.
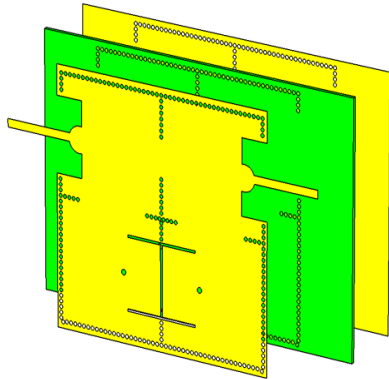
PEC	
Ro4003	

Fig. 4. Configuration of the proposed structure.

IV. RESULTS OF THE DESIGN

The S-parameter parameter frequency response (S_{11}) of the designed SIW fourth-order structure is evident in Fig. 5. According to Fig.5, the central frequency of the designed SIW fourth-order filter is set at 5.5 GHz. The bandwidth of the designed SIW filter is approximately 0.7 GHz. The filter poles are at 5.226, 5.5255, and 5.6726 GHz, respectively. Return loss is reported at about 30.2 dB. The insertion loss is about 1.9 dB.
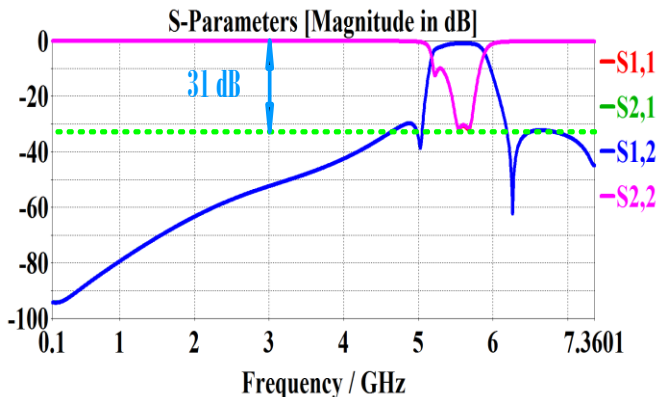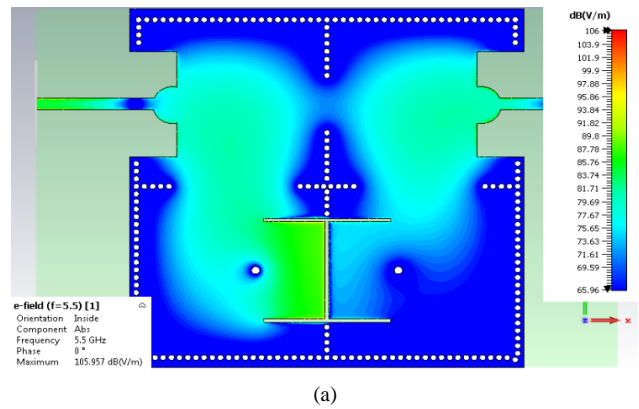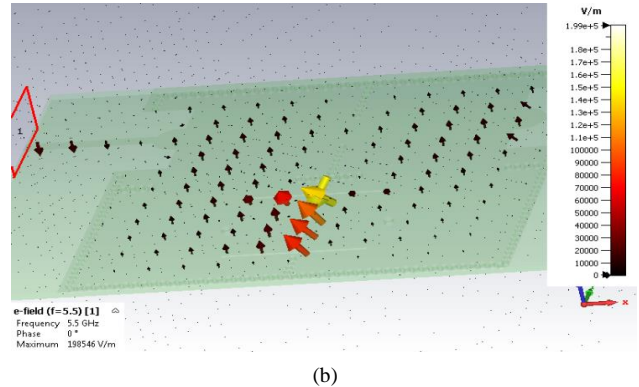

Fig. 5. Wideband frequency response.

Fig. 5, which shows the wideband frequency response, indicates that the 31-dB rejected level until 7.4 GHz. The distribution of Forth order SIW filter E- field lines is illustrated in Fig. 6.
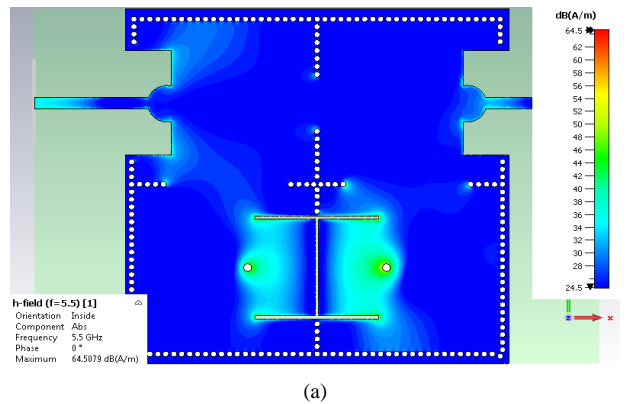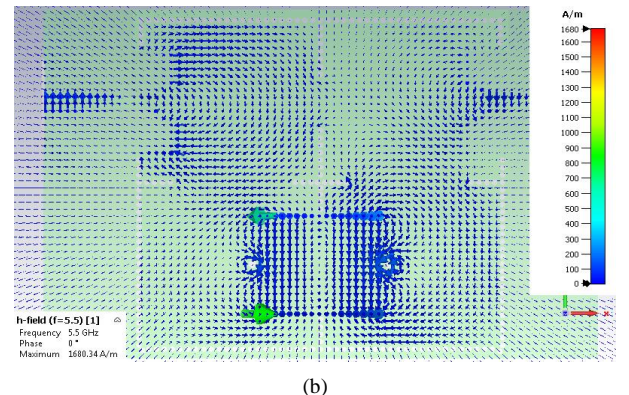

(a)

(b)

Fig. 6. E-field distribution in central frequency ($f_0 = 5.5\ GHz$).

The H- field distribution diagram of the proposed filter structure is presented in Fig. 7.

(a)

(b)

Fig. 7. H-field distribution in central frequency ($f_0 = 5.5\ GHz$).

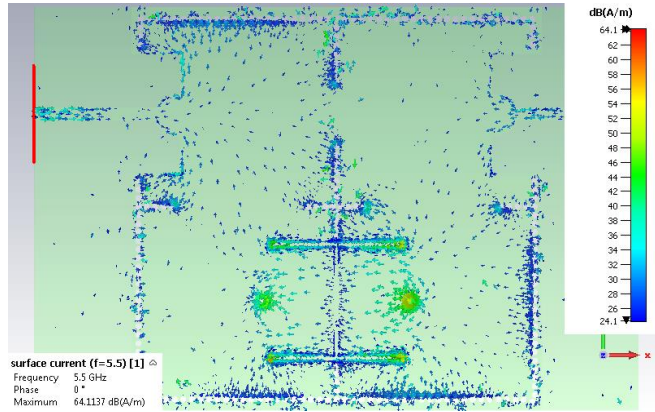In Fig. 8, the distribution diagram of the surface current of the quasi-elliptic filter is shown.

Fig.8. Distribution diagram of the surface current in central frequency ($f_0 = 5.5\ GHz$).

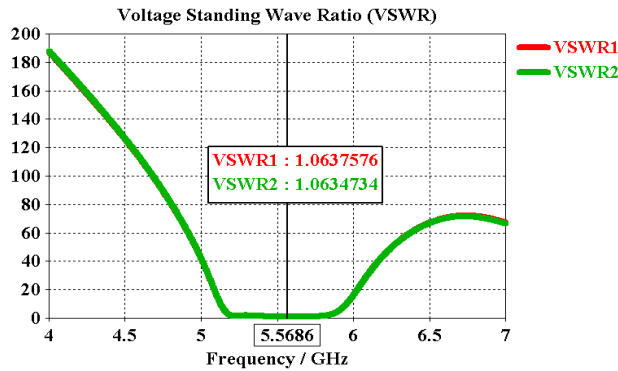The VSWR curve is shown in Fig. 9 and provides excellent results.

Fig. 9. VSWR of the proposed SIW filter.
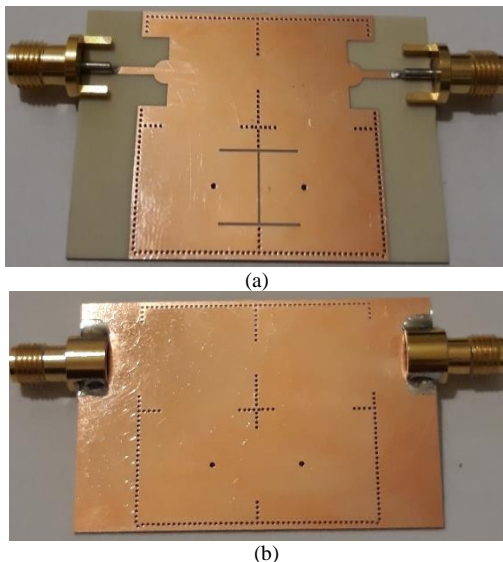

(a)

(b)

Fig. 10. The form of the fabricated fourth-order SIW filter, (a) Top view, (b) Bottom view.

V. FABRICATION RESULTS

The prototype of the fabricated SIW fourth-order filter is displayed in Fig. 10.

The results of the frequency response curve measurement of the fourth-order SIW filter structure by the Network Analyzer are shown in Fig. 11.
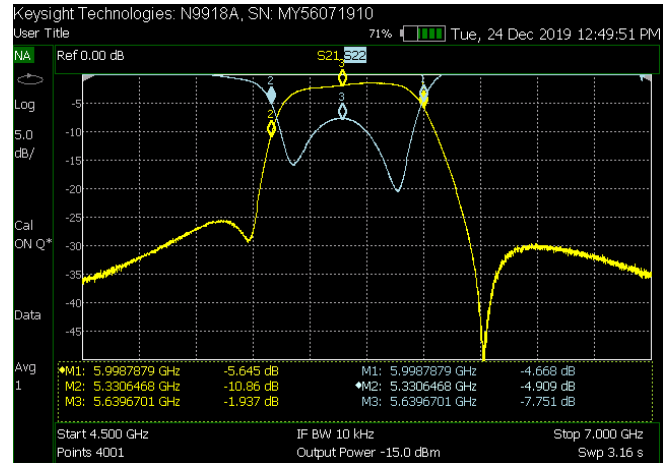

Fig. 11. The measurement results of the fabricated SIW filter.

As seen in Fig. 11, there is a cooperative agreement between the measurement results and the simulation, confirming of each.

A comparison of the performance of the designed filter structure and similar presented structures in other articles are shown in Table II.

TABLE II

Comparison of the Designed Filter with Other Articles in This Field.

References	BW_{3dB} (GHz)	f_0 (GHz)	Filter Order	IL (dB)	Number of TZs	FBW	Rejection	Size $(\lambda_g)^2$
[3]	0.2	4.99	3	1.5	2	5	Null	1.25
[4]	0.3	3.6	3	1.35	2	9.7	$20/1.99f_0$	0.63
[5]	0.55	20	4	2.78	1	2.75	50/1.49	2.53
[6]	0.6	13.2	2	1.5	1	4.55	$20/2.3f_0$	0.47
[7]	0.7/ 0.5	10	3	2.91	1	1.51	$25/2.1f_0$	1.86
[8]	-	10	2	0.8	2	1	-	3
Presented work	0.7	5.5	4	1.9	2	12.73	$31/1.4f_0$	0.65

VI. CONCLUSION

In this proposed paper, a compact fourth-order quasi-elliptic filter has been studied. Various electric and magnetic couplings have been used to implement the structure of this filter. Studies of filter coupling configuration have been fully reported. SIW technology implements this filter. The advantages of using SIW in this structure were low loss, low cost, and easy construction. The quasi-elliptic filter has been designed in the C band. The central frequency of the designed SIW fourth-order filter was set at 5.5 GHz. The bandwidth of the designed SIW filter was approximately 0.7 GHz. The filter poles were at 5.226, 5.5255, and 5.6726 GHz, respectively. Return loss was reported at

about 30.2 dB. The insertion loss was about 1.9 dB. There was a good agreement between the fabrication results and the simulation.

Ⅶ. ACKNOWLEDGMENT

Ⅷ. REFERENCES

[1] Kiani N, Afsahi M. Design and fabrication of a compact SIW diplexer in C-band. Iranian J. Electr. Electron. Eng. 2019;15 (2):189–194.

[2] Kiani N, Tavakkol Hamedani F, Rezaei P. Implementation of a reconfigurable miniaturized graphene-based SIW antenna for THz applications. Micr. Na. 2022.

[3] Wu LS, Zhou XL, Wei QF, Yin W. An extended doublet substrate integrated waveguide (SIW) bandpass filter with a complementary split ring resonator (CSRR), IEEE Microw. Wireless Compon. Lett. 2009;19 (12): 777–779.

[4] Shen W, Yin WY, Sun XW. Compact substrate integrated waveguide transversal filter with microstrip dual-mode resonator. J. Electromagn. Waves. Appl. 2010;24 (14): 1887–1896.

[5] Zhu F, Hong W, Chen JX, Wu K. Wide stopband substrate integrated waveguide filter using corner cavities. Electron. Lett. 2013;49 (1): 50–52.

[6] Jia D, Feng Q, Xiang Q, Wu K. Multilayer substrate integrated waveguide (SIW) filters with higher-order mode suppression. IEEE Microw. Wireless Compon. Lett. 2016;26 (9): 678–680.

[7] Zhou K, Zhou CX, Wu W. Resonance characteristics of the substrate-integrated rectangular cavity and their applications to dual-band and wide-stopband bandpass filter design. IEEE Trans. Microw. Theory Techn. 2017;65 (5): 1511–1524.

[8] Kiani S, Rezaei P, Karami M, R.A. Sadeghzadeh. Substrate integrated waveguide quasi-elliptic bandpass filter with parallel coupled microstrip resonator. Electron. Lett. 2018; 54: 667–668.

[9] Simsek S, Rezaeieh SA. A design method for substrate integrated waveguide electromagnetic bandgap (SIW-EBG) filters. AEU Int. J. Electron. Commun. 2013;67:981–983.

[10] Moitra S, Bhowmik PS. Modeling and analysis of Substrate Integrated Waveguide (SIW) and half-mode SIW (HMSIW) band-pass filter using reactive longitudinal periodic structures. AEU Int. J. Electron. Commun. 2016;70:1593–1600.

[11] Aghayari H, Nourinia J, Ghobadi C, Mohammadi B. Realization of dielectric-loaded waveguide filter with substrate integrated waveguide technique based on the incorporation of two substrates with different relative permittivity. AEU Int. J. Electron. Commun.2018;86:17–24.

[12] Martínez J, Coves Á, Bronchalo E, San Blas ÁA, Bozzi M. Band-pass filters based on periodic structures in SIW technology. AEU Int. J. Electron. Commun. 2019;112:152942.

[13] Máximo-Gutiérrez C, Hinojosa J, Alvarez-Melcon A. Design of wide band-pass substrate integrated waveguide (SIW) filters based on stepped impedances. AEU Int. J. Electron. Commun.2019;100:1–8.

[14] Wang X, Zhang D, Liu Q, Deng H, Lv D. Tunable bandpass filter with a wide tuning range of center frequency and bandwidth based on circular SIW. AEU Int. J. Electron. Commun.2020;114:153002.

[15] Huang L, Wu W, Zhang X, Lu H, Zhou Y, Yuan N. A novel compact and high-performance bandpass filter based on SIW and CMRC techniques. AEU Int. J. Electron. Commun.2017;82:420–425.

[16] Parameswaran A, Raghavan APS. Miniaturizing SIW filters with slow-wave technique. AEU Int. J. Electron. Commun.2018;84:360–365.

[17] Aghayari H, Nourinia J, Ghobadi C. Incorporated substrate integrated waveguide filters in propagative and evanescent mode: realization and comparison. AEU Int. J. Electron. Commun.2018;91:150–159.

[18] Meiguni JS, Ghobadi Rad A. WLAN substrate integrated waveguide filter with novel negative coupling structure. J. Model. Sim. Electr. Electron. Eng. 2015;1 (2):15–18.

[19] Amn-e-Elahi A, Rezaei P. SIW corporate-feed network for circular polarization slot array antenna. Wireless Pers. Commun. 2020;111: 2129–2136.

[20] Meiguni JS, Pommerenke A. Theory and experiment of UWB archimedean conformal spiral antennas. IEEE Trans. Antennas Propag. 2019;67 (10): 6371–6377.

[21] Meiguni JS, Kamyab M, Hosseinbeig A. Theory and experiment of spherical aperture-coupled antennas. IEEE Trans. Antennas Propag. 2013;61 (5): 2397–2403.

[22] Wang B, Cappelli MA. A tunable microwave plasma photonic crystal filter. Appl. Physic. Lett. 2015; 107(17): 171107.

[23] Pal B, Mandal MK, Dwari S. Varactor tuned dual-band bandpass filter with independently tunable band positions. IEEE Microw. Wireless Compon. Lett. 2019; 29(4): 255–257.

[24] Zhu H, Abbosh A. Compact tunable bandpass filter with a wide tuning range of center frequency and bandwidth using coupled lines and short-ended stubs. IET Microw. Antennas Propag. 2016; 10(8): 863–870.

[25] Xiao JK, Su XB, Wang HX, Ma JG. Compact microstrip balanced bandpass filter with adjustable transmission zeros. Electron. Lett. 2019; 55(4): 212–214.

[26] CST GmbH, Germany, CST STUDIO SUITE Ver. 2015 – User's Manual, Dec. 2015. www.cst.com.

[27] Cameron RJ. General coupling matrix synthesis methods for Chebyshev filtering functions. IEEE Trans. Microw. Theory Tech. 1999; 47 (4): 433–442.

[28] Cameron RJ. Advanced coupling matrix synthesis techniques for microwave filters. IEEE Trans. Microw. Theory Tech. 2003; 51 (1): 1–10.

[29] Hong JS. Lancaster MJ. Microstrip filter for RF/microwave applications. New York: Wiley, 2001: 235–272.